13

Assessment of Rodent Glioma Models Using Magnetic Resonance Imaging Techniques

Rheal A. Towner, Ting He, Sabrina Doblas and Nataliya Smith
Advanced Magnetic Resonance Center, Oklahoma Medical Research Foundation
Oklahoma City
U.S.A.

1. Introduction

There is a strong need to obtain precise surrogate biomarkers to improve the accuracy of diagnosis for gliomas, and to effectively evaluate therapeutic response. Often pre-clinical models of disease are used to develop diagnostic procedures and assess the effectiveness of a potential therapy. For gliomas, there are a variety of rodent models that have been investigated by numerous investigators over the past few decades, ranging from intracranial rodent glioma cell implantation models, intracranial human glioma xenografts, orthotopic implantation of human glioma stem cells, multipotent human glioblastoma stem-like neurosphere lines, transgenic mouse models, to viral-induced progenitor or stem cell derived glioma models. Tumor grades in these models vary from low to high grade tumors, with many of the high-grade glioma models sharing some of the characteristics of human grade IV glioblastoma multiforme (GBM). Many of the characteristic features of gliomas can be assessed diagnostically with *in vivo* imaging techniques such as magnetic resonance imaging (MRI). MRI has the capability of obtaining morphological/anatomical, functional, biophysical, molecular and metabolic information of a disease at various pathological stages of development. Tumor characteristics often associated with aggressive gliomas include an invasive growth pattern, angiogenesis, necrosis, hypoxia, edema, and alterations in major metabolic pathways. Morphological features, such as tumor size and position, infiltrative growth, hemorrhaging, necrotic lesions, edema, mass effect, heterogeneity, and cyst formation, can be followed using standard contrast-enhanced T_1-weighted MR imaging or non-contrast T_2-weighted imaging.

Although conventional MRI provides us with some indication about the nature of the lesion or tumor, it has limited sensitivity and specificity in determining histological type and grade, delineating margins and differentiating edema, as well as effectively evaluating therapeutic effects or side-effects. Incorporating some advanced MR techniques, such as MR angiography (MRA), perfusion-weighted MR imaging (PWI), diffusion-weighted MR imaging (DWI), MR spectroscopy (MRS), and molecular MRI (mMRI), may help to overcome some of those limitations. Angiogenesis associated with major blood vessels can be assessed using MR angiography, whereas perfusion-weighted imaging can be used to monitor angiogenesis associated with capillary vessels in tumors. Biophysical parameters such as water diffusion, as measured by diffusion-weighted imaging, have also provided

information regarding alterations in tissue structure associated with glioma tumors. An extension of the diffusion-weighted imaging technique is diffusion tensor imaging (DTI), which can provide information on white matter neuronal fiber tractography. MR spectroscopy can be used to assess alterations in tumor metabolites associated with glucose, bioenergetics, amino acid or lipid metabolism, for example. Many of these advanced MR techniques are used in a clinical setting. More recently, molecular MRI (mMRI) which incorporates a MRI contrast agent as a signaling molecule and an affinity component that targets specific tumor markers associated with tumor growth, angiogenesis, cell invasion, inflammation, or apoptosis, can be used to characterize *in vivo* molecular events associated with gliomas.

This review will focus on various glioma models that have been studied *in vivo*, with particular emphasis on MR image and/or spectroscopy evaluation of these models, and the use of MR image criteria (morphological, biophysical, molecular and metabolic) to evaluate therapeutic treatments. The aims are to: (1) provide an overview on current rodent glioma models being studied; (2) provide an overview regarding currently used MR methods, including advanced MR techniques (e.g. MRA, DWI, PWI, MRS and mMRI), relevant to glioma research; and (3) summarize studies that have used MR methods to evaluate therapeutic response in pre-clinical models for gliomas.

2. Human gliomas

Gliomas represent 40% of all primary central nervous system (CNS) tumors diagnosed. Among them, glioblastomas (GBM) are the most malignant, with a very poor survival time of about 15 months for most patients diagnosed with this grade IV brain tumor (CBTRUS 2011). High grade gliomas are the most common primary brain tumors in adults, and their malignant nature ranks them as the fourth largest cause of cancer death (Niclou *et al*., 2010). There are four tumor grades for gliomas: Grade I which is a non-malignant, fairly circumscribed astrocytoma that is rare and appears in young adults; Grade II which are a more common diffusely infiltrating astrocytoma; Grade III which is an anaplastic astrocytoma; and Grade IV which is a glioblastoma multiforme (Niclou *et al*., 2010). Grades II-IV gliomas generally are found in the adult population, and often recur following current treatment options (including surgical resection, radiotherapy, and chemotherapy) (Niclou *et al*., 2010).

Grading and identification criteria that can be used to provide information regarding tumor behavior are cell proliferation (cellularity and mitotic activity), nuclear atypia, neovascularization and the presence of necrosis and/or apoptotic regions (Gudinaviciene *et al*., 2004). Grade II gliomas (also referred to as diffuse astrocytomas) and grade III gliomas (also referred to as anaplastic astrocytomas) only differ based on their mitotic activity, and this difference accounts for a substantial decrease in the 5-year survival for patients, from 47% to 29% (from grade II to III, respectively) (CBTRUS 2011). Grade IV gliomas (GBM) are often characterized by the presence of large necrotic areas (Gudinaviciene *et al*., 2004) and generally have a 3% 5-year survival (CBTRUS 2011).

3. Rodent models of gliomas

Animal models are often used when researching a disease and trying to understand how a particular pathological process occurs, as well as a means of studying the efficacy of

potential new therapies. This review will provide examples of commonly used and new experimental animal models for gliomas, which make up a large portion of primary brain tumors. The majority of models involve intracerebral implantation of rodent (rat or mouse) or human glioma cells into synergetic rats or mice, or immunocompromised rodents (e.g. nude or athymic rats or mice). There are also a limited number of transgenic mouse models for gliomas. One approach to better simulate a human tumor is to obtain human glioma neurospheres from patients during tumor resection, and then culture the cells prior to intracerebral implantation into immunocompromised rodents. Another recent approach is to implant non-replicating viruses that can stimulate neuronal stem cells to turn into glioma cells which develop into diffuse tumors similar to those found in high-grade or malignant gliomas called, glioblastoma multiforme (or GBM).

3.1 Intracerebral cell implantation models

Glioma cells (rat, mouse or human origin) are injected into the cerebral cortex of rats or mice (synergetic if cells are transplanted into the same species and strain that they were obtained from, or immune-compromised rats or mice if human cells are used) using a stereotaxic device for precise implantation into a brain region. As tumors grow over a period of 1-2 months, this model is considered a short-term model. Different cell lines varying in their degree of malignancy, such as rat C6, 9L/LacZ, F98 and RG2 cells, mouse GL261 cells and human U87 cells, provide a range of gliomas from moderately aggressive to GBM-like.

Many of these models have some characteristics associated with human gliomas, such as aggressive tumor growth, angiogenesis, and tumor necrosis (in a few models), however the diffuse nature of high-grade gliomas, glioblastoma multiforme (GBM), is not well represented. In many instances the intracerebrally-implanted rodent tumors have defined tumor boundaries, which do not represent the infiltrative nature of GBMs well. A comprehensive review that discusses the advantages and disadvantages of rat brain tumor models, most of them involving intracerebral implantation of rat glioma cells, is discussed in a paper by Barth and Kaur (2009).

The rat C6 cell line produces diffusively invasive astrocytomas (Barth, 1998; Barth and Kaur, 2009), which have been found to be similar to human glioma cells regarding the expression of genes mainly involved in tumor progression (Sibenaller *et al*., 2005). C6 gliomas were induced in an outbred Wistar rat strain repeatedly injected with methylnitrosourea (MNU), which makes it non-syngeneic in inbred strains, and increases its potential to evoke an alloimmune response (Barth and Kaur, 2009). As a result of some genetic similarities to human gliomas, the C6 model has been widely used as a GBM model for a number of years (Grobben *et al*., 2002; Barth and Kaur, 2009). The 9L/LacZ-derived tumors are aggressive and infiltrative, and are angiogenic (Plate *et al*., 1993), which are some of the characteristics associated with human GBM (Weizsaecker *et al*., 1981). Although the aggressive 9L/LacZ gliomas are highly invasive (Szatmori *et al*., 2006) and have extensive neovascularization (Plate *et al*., 1993), due to their pronounced immunogenicity (Barth, 1998) and the fact that they are classified as gliosarcomas (Sibenaller *et al*., 2005), makes these cells a poor choice for glioma studies. F98 gliomas are classified as anaplastic malignant tumors, which have an infiltrative pattern of growth, and also have attributes associated with human GBM (Barth, 1998; Barth and Kaur, 2009). The aggressive and invasive nature (Barth, 1998; Barth and Kaur, 2009) of RG2 tumors (Groothuis *et al*., 1983), as well as the highly tumorigenic human glioblastoma U87 MG cell line *(Martens et al*., 2006; Cheng *et al*., 1996), both mimics human

high-grade gliomas via inducing vascular alterations. U87 pcDNA3 and U87 IRE1 DN human glioma cells were selected as malignant glioma models that form highly versus poorly vascularized tumors, respectively (Drogat *et al*., 2007; Wehbe *et al*., 2010). GL261 cells give rise to quickly growing, and diffusively invasive intracranial tumors in C57BL/6 mice (Szatmori *et al*., 2006). RG2 and F98 glioma cell lines were both obtained from chemical induction as a result of administering ethylnitrosourea (ENU) to pregnant rats, where the progeny developed brain tumors that were isolated, and propagated and cloned in cell culture (Barth and Kaur, 2009). Human U87 cells are of high interest for angiogenesis studies (Cheng *et al*., 1996). The immunogenicity issue of the 9L/Lacz model can be resolved by using non-immunogenic models (e.g. RG2).

Xenograft models, induced by orthotopic (into native tumor sites) injection of primary tumor cells or tumor cell lines, represent the most frequently used *in vivo* cancer model systems for glioma research (Waerzeggers *et al*., 2010). Both cell culture and xenograft model systems lack the stepwise genetic alterations that are thought to occur during tumor progression, and often do not represent the genetic and cellular heterogeneity of primary tumors, as well as the complex tumor-stroma interaction (Waerzeggers *et al*., 2010). Genetically engineered mouse models (discussed below in the "Transgenic Mouse Models" section) better represent the causal genetic events and subsequent *in situ* molecular evolution, the tumor-stroma interactions, and consist of cellular subpopulations such as cancer stem cells (discussed further in the "Human Glioma Neurospheres" and "Viral-Induced Glioma Models" sections below), that occur in native tumors (Waerzeggers *et al*., 2010).

3.2 Chemical-induced model

Slow-growing, low- and high-grade, spontaneous gliomas can be generated with a chemically-induced model from the administration of ENU (Kish *et al*., 2001; Koestner, 1990). Transplacental ENU exposure of a pregnant female a day before gestation, results in the formation of low-grade oligodendrogliomas and mixed gliomas, with a tumor incidence approaching 100%, in rat pups at approximately 3-6 months of age (Koestner, 1990). In addition to oligodendrogliomas and mixed gliomas, unfortunately the ENU-induced model also results in the formation of meningiomas (Koestner *et al*., 1971), spinal cord tumors (Koestner *et al*., 1971) and other primitive neuroectodermal tumors (Vaquero *et al*., 1992), decreasing its potential as a reproducible model. In addition to the isolation of RG2 and F98 rat glioma cells from ENU induction, A15A5 neoplastic astrocytes have also been cloned (Davaki and Lantos, 1980).

3.3 Transgenic mouse models

As we are beginning to understand the genetic mutations associated with gliomas, it is possible to generate transgenic mouse models that have these genetic mutations. Recent findings suggest that brain tumors originate from neural stem or progenitor cells. Some examples of transgenic mutations include deletions of gene combinations, such as Rb/p53, Rb/p53/PTEN or PTEN/p53 (Jacques *et al*., 2010). pRb is a retinoblastoma protein, which is a tumor suppressor protein that is dysfunctional in many cancers. Rb controls excessive cell growth by inhibiting cell cycle progression until the cell is ready to divide (Chinnam and Goodrich, 2011; Lohmann, 2010). p53 which is also known as protein 53 is a tumor suppressor protein responsible for regulating the cell cycle (Kim et al., 2011; Maclaine and

Hupp, 2011; Muller et al., 2011). PTEN, which stands for phosphatase and tensin homolog, is a tumor suppressor gene also involved in the regulation of the cell cycle (Natsume et al., 2011; Alexiou and Voulgaris, 2010). Rb/p53 mice developed malignant tumors in approximately 9 months (Jacques *et al*., 2010). PTEN/Rb/p53 tumors had an appearance that was similar to the Rb/p53 tumors (Jacques *et al*., 2010). Deletion of Rb/p53 or Rb/p53/PTEN resulted in the formation of primitive neuroectodermal tumors (PNET), which alludes to the role of an initial Rb loss involved in driving the PNET phenotype (Jacques *et al*., 2010). It was found that targeted deletion of PTEN and p53 in subventricular zone (SVZ) stem cells resulted in glioma formation with a latency period of approximately 7-8 months (Jacques *et al*., 2010). The tumors from the recombination of PTEN/p53 were histologically infiltrative, diffuse, necrotic and had signs of micro-vascular proliferation, which are all characteristics of human high-grade gliomas (Jacques *et al*., 2010).

Another successful transgenic mouse model involves the deletion of the *TP53* (tumor protein 53) gene (*Trp53 null* background), and over-expressing human PDGF (platelet-derived growth factor) under the control of the GFAP (glial fibrillary acidic protein) promoter, which developed tumors with human glioblastoma-like features and with the integrated development of PDGFRα$^+$ tumor cells and PDGFRβ$^+$ Nestin$^+$ vasculature in 2-6 months (Hede *et al*., 2009). The tumor suppressor gene *TP53* is either lost or commonly mutated in astrocytic brain tumors, and these *TP53* alterations are often combined with excessive growth factor signaling via the PDGF/PDGFRα complex (Hede *et al*., 2009). PDGF is one of many growth factors that regulate cell growth and division, and has been found to be widely associated with malignant gliomas (Calzolari and Malatesta, 2010; Shih and Holland, 2006).

4. Human glioma neurospheres

GBM cancer-initiating cells have been found to mediate resistance to chemotherapy and radiation treatment, both used as follow-up therapies following surgical resection of the main tumor mass (Wei *et al*., 2010). Cells isolated from GBM that possess the capacity for self-renewal following radiation and chemotherapy, can form neurospheres when cultured *in vitro* (Wei *et al*., 2010). The glioma-associated cancer-initiating cells were found to express MHC-I (major histocompatibility I) but not MHC-II, CD-40 or CD80, which induces T-cell immune deficiency, and express the costimulatory inhibitory molecule, B7-H1, which plays a role in mediating immune resistance in gliomas and induces T-cell apoptosis (Wei *et al*., 2010). These neurospheres can be intracerebrally implanted into immune-compromised rodents to develop tumors *in vivo,* and therefore provide an experimental model that more closely resembles recurrent human GBM (radiation and chemotherapeutic resistant and induce immunosuppression) to evaluate new therapies. Another approach that takes into consideration the role of tumor-initiating stem cells, is to orthotopically implant tiny fragments of surgically-resected tumors, containing brain tumor stem cells within the glioblastoma tissue, into immunocompromised mice (xenograft model) brains with the use of a trocar system (Fei *et al*., 2010).

4.1 Viral-induced glioma models

Glial progenitor cells in the white matter and subventricular zone within the central nervous system were recently found to be the likely candidates for glioma-initiating cells (Assanah *et*

al., 2006, 2009; Masui *et al*., 2010). Intracerebral implantation of PDGFB-green fluorescent protein (GFP)-expressing retroviruses into rodents were found to induce tumors that closely resembled diffuse human malignant gliomas which have been challenging to treat (Assanah *et al*., 2006; Masui *et al*., 2010). This model involves the use of a viral vector that stimulates neuronal stem cells to become glioma cells by expressing PDGF, which is involved in generating tumor cells (Masui *et al*., 2010). These studies demonstrate that both adult white matter and glial progenitors generate gliomas, as well as recruit resident progenitors to proliferate within the mitogenic environment of a tumor, and therefore contributing to the heterogeneous mass of cells that make up a malignant glioma (Assanah *et al*., 2006; Masui *et al*., 2010). It was previously demonstrated that PDGF-B could play a dose-dependent role in glial tumorigenesis, where PDGFR (PDGF receptor) signaling via elevating levels of PDGF-B chain expression quantitatively regulates tumor grade, and that PDGF-B expression is required to sustain high-grade oligodendrogliomas (Shih *et al*., 2004). PDGF-B expression in tumor cells was elevated by removing inhibitory regulatory elements in the *PDGFB* mRNA and a retroviral delivery system (Shih *et al*., 2004). To generate tumors, DF1 cells transfected with RCAS (repeat with splice acceptor) retroviral vectors, generating a culture of virus-producing cells, were injected intracranially into N-tva transgenic mice (Shih *et al*., 2004). By inhibiting PDGFR activity, it was possible to convert tumors from high to low grade (Shih *et al*., 2004).

Another recent study involved intracranial injection of lentiviral vectors with GFAP (glial fibrially acidic protein) or CMV (cytomegalovirus) vectors into compound *LoxP*-conditional mice, which resulted in K-Ras^{v12} expression and loss of p16^{Ink4a}/p19^{Arf}, with or without concomitant loss of p53 or Pten (de Vries *et al*., 2010). Like GFAP, CMV is a promoter (de Vries *et al*., 2010). CMV-Cre injection into *p53;Ink4a/Arf;K-Ras^{v12}* mice was particularly found to result in the formation of high-grade gliomas within 2-3 weeks that had invasiveness and blood-brain barrier functionality characteristics that are found in human high-grade gliomas (de Vries *et al*., 2010).

5. MRI methods to detect gliomas

Magnetic resonance imaging (MRI) techniques are becoming more commonly used to provide information on brain tumor growth, vasculature, biochemical metabolism, and molecular changes in preclinical models, as MRI is the optimal imaging tool as part of the diagnostic process for human gliomas. Conventional MRI techniques, such as T_1- and T_2-weighted imaging, contrast-enhanced T_1-weighted imaging, dynamic contrast enhanced (DCE) imaging, and diffusion-weighted imaging (DWI) methods can provide useful information on tumor location and extent of growth, blood-brain barrier (BBB) disruption, brain invasiveness, regional blood flow and blood volume, and tumor cellularity, all of which are characteristics associated with glioma grade and prognosis in a clinical setting (Waerzeggers *et al*., 2010).

Morphological MRI (T_2-weighted or T_1-weighted contrast-enhanced imaging) is used to provide information on tumor volumes and growth rates, which can be used to distinguish between tumor grades. Contrast-enhanced imaging can be used to assesses BBB disruption, however this feature can be absent in diffuse infiltrative tumor regions or when assessing therapeutic treatment (Waerzeggers *et al*., 2010). DCE imaging can be used to follow tumor angiogenesis by measuring changes in tumor vascular permeability, vascular density and

vessel morphology (Waerzeggers *et al*., 2010), particularly regarding the capillary bed. Magnetic resonance angiography (MRA) is also used to provide information on tumor vasculature associated with angiogenesis, however it tends to be restricted to major blood vessels >50 microns in diameter (Doblas *et al*., 2010). DWI has been used in cancer imaging to evaluate tumor cellularity and infiltration, as well as monitor therapeutic response (Kauppinen, 2002). Metabolic information can be obtained by monitoring tumor metabolites by a method called MR spectroscopy (MRS), or variations thereof, such as MR spectroscopic imaging (MRSI) or chemical shift imaging (CSI). Molecular alterations can be assessed with the use of targeting MR contrast agents which can specifically indicate levels of cancer biomarkers that may be elevated in malignant tumors. The development of targeted imaging ligands attached to MRI contrast agents allows the *in vivo* evaluation of tumor biology, such as tumor cell apoptosis, angiogenic blood vessels or the expression of specific tumor antigens or signaling pathways (Waerzeggers *et al*., 2010).

5.1 Tumor morphology

MRI is obtained on small animal MR imaging systems (7 - 11.7 Tesla), that can accommodate rodents such as mice and rats. MR images are obtained in multiple slices (0.5-1 mm thick) to visualize an entire tumor (Gartesier *et al*., 2010). Examples of rodent tumor models for gliomas (e.g. rat C6 and RG2 models, and mouse GL261 model) are shown in Figure 1, depicting heterogeneous tumors (right cerebral cortex, upper regions) following intracerebral (orthotopic) implantation of rat or mouse glioma cells (Doblas *et al*., 2010).

From the multiple image slices through a tumor, tumor volumes can be measured, and the growth rate can be calculated from multiple imaging sessions over several days, weeks or months (as shown in Figure 2). Tumor areas are traced in multiple slices to calculate tumor volumes, which can be used to determine tumor growth and doubling times (Doblas *et al*., 2008, 2010; Garteiser *et al*., 2010). Robust tumor volume determinations can be made by using manual or automated segmentation techniques, which can be used to delineate tumor margins on the basis of signal intensity differences from surrounding brain tissue (Waldman *et al*., 2009).

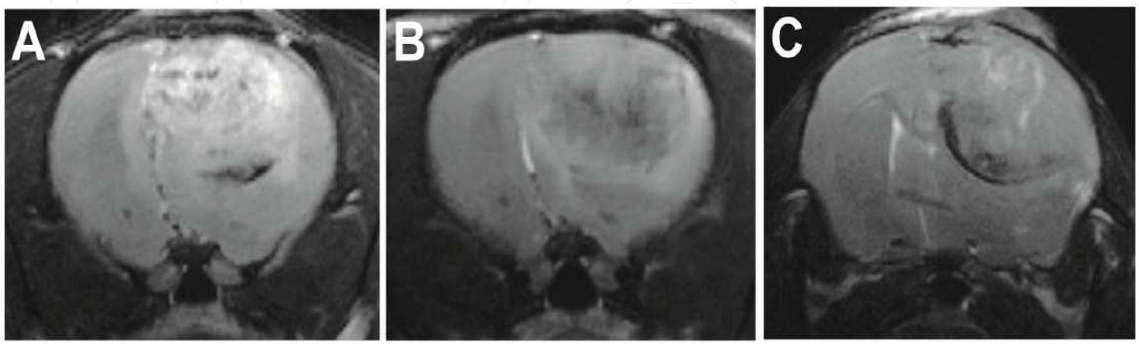

Fig. 1. MR images of rodent gliomas. T_2-weighted images of the rat C6 (A; 18 days following intracerebral implantation of cells) and RG2 (B; 13 days following cell implantation), and the mouse GL261 (C; 26 days following cell implantation) glioma models. Tumors appear as heterogeneous regions in the upper right area of the cerebral cortex regions.

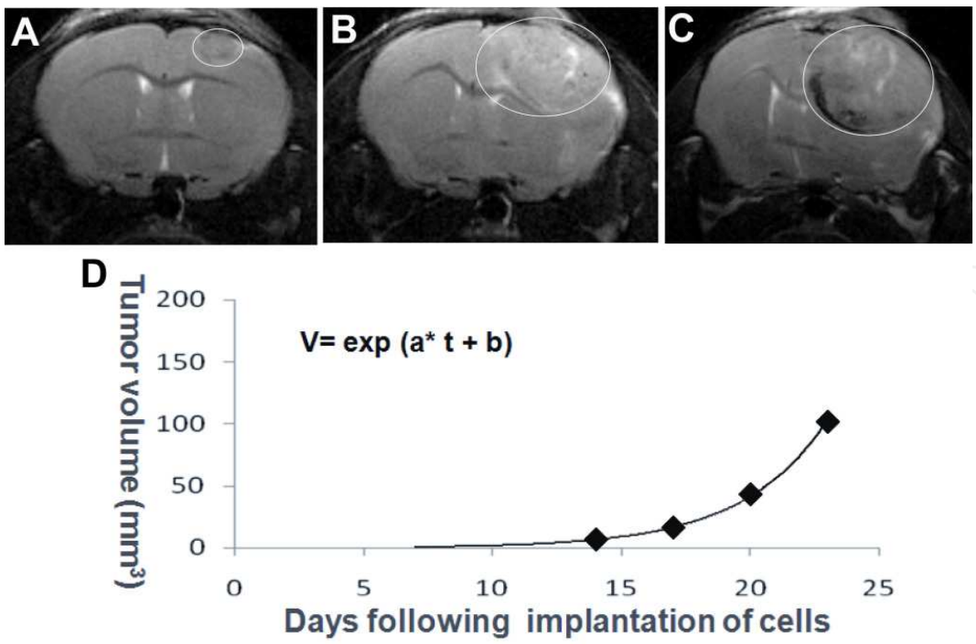

Fig. 2. MR images used to calculate tumor volumes and tumor growth. T_2-weighted images of a mouse GL261 glioma at 14 (A), 23 (B) and 26 days (C) following intracerebral implantation of cells. Tumors are outlined (white ellipses). (D) Calculated GL261 tumor volumes which follow an exponential increase over time.

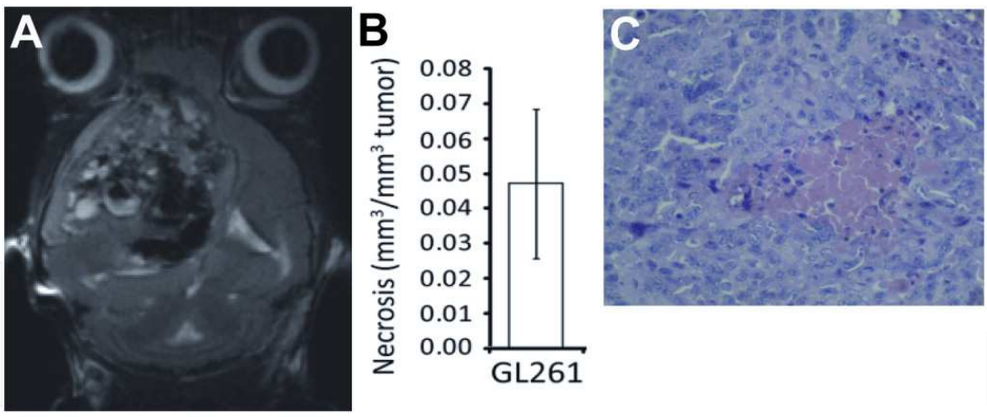

Fig. 3. Determination of necrotic volumes from MR image-observed tumors. (A) T_2-weighted MR image of a GL261 mouse glioma at 23 days following intracerebral implantation of cells. Note dark void regions in the heterogeneous tumor which are necrotic lesions. (B) Necrotic volumes from tumors can be measured (n=5; mean±S.D.). (C) Corresponding histological slide depicting necrosis in a GL261 tumor.

Tumor morphology can also provide information on tumor invasiveness and necrotic lesions. Necrotic lesions are depicted as dark void regions in a tumor (as shown in Fig. 3A), of which volumes (e.g. Fig. 3B) can be measured from multiple slices (Towner *et al*., 2010a). A comparison between the orthotopic rat glioma models, C6 and RG2, and the chemical

ENU-induced model, indicated that percent necrosis was highest in the ENU model, compared to RG2, and least in the C6 model (Towner *et al*., 2010a). Although the ENU-induced model is used to generate low-grade gliomas, it generates a heterogeneous population of glioma cells ranging from low- to high-grade, which contributes to the high incidence of necrotic lesions (Towner *et al*., 2010a). RG2 gliomas are known to be more aggressive, invasive and infiltrative than C6 gliomas (Groothuis *et al*., 1983). It has also been shown that RG2 gliomas have more diffuse margins at the interface to adjacent brain tissue, whereas C6 gliomas are less infiltrative with a distinct peritumoral region at the margin of the tumor (Doblas *et al*., 2010).

5.2 Tumor vasculature and ultrastructure

MR angiography can provide information on new blood vessels formed in tumors, a process known as angiogenesis which is required to maintain tumor growth. On small animal imaging MRI systems, the image in-plane resolution is >50 μm, which allows visualization of major blood vessels, arterioles and venules (Doblas *et al*., 2008, 2010). Quantitation of brain and tumor blood vessels can also be obtained, as well as measurements on blood vessel diameters and lengths (Doblas *et al*., 2008, 2010). An increase in total brain tumor blood volume was found to directly correlate with increasing tumor volumes during tumor growth (Doblas *et al*., 2010).

Quantification of the Brownian motion of water or diffusion within tissues can be measured through the apparent diffusion coefficient (ADC) which is obtained from diffusion-weighted imaging datasets. DWI yields ultrastructural information on cellular density and the extracellular matrix (Waldman *et al*., 2009; Sadeghi *et al*., 2003). Figure 5 shows an example of an ADC (Fig. 5 b) map in a C6 glioma-bearing rat brain, indicating higher ADC values in tumor tissue compared to contralateral 'normal' brain tissue (Garteiser *et al*., 2010).

Temporal diffusion spectroscopy based on oscillating gradient spin-echo (OGSE) MRI was used to detect microscopic structural variations at the subcellular scale in C6 rat gliomas

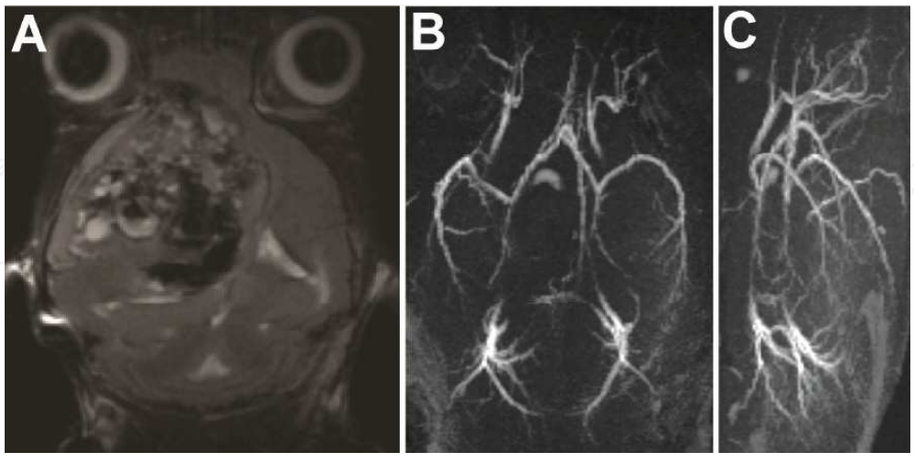

Fig. 4. MR angiography of a GL261 mouse glioma. (A) T_2-weighted MR image of a GL261 glioma-bearing mouse brain (23 days following intracerebral implantation of cells.) (B) and (C), 3 dimensional angiograms of mouse brain blood vessels of a GL261 glioma-bearing mouse. Note altered vasculature on left-hand side in image B, as well as increased blood vessels (middle cerebral artery; depicted in left-mid-region of image C) in the tumor region.

Fig. 5. Diffusion- and perfusion-weighted imaging of a rat C6 glioma. (A) T_2-weighted MR image of a C6 glioma-bearing rat brain (20 days following intracerebral implantation of cells). (B) ADC map (1×10^{-4} mm^2/s) of a C6 glioma. Note higher ADC values in the tumor compared to 'normal' brain tissue. (C) Perfusion map (ml/(100g×min)) in a C6 glioma. Note decreased perfusion values in tumor tissue, compared to 'normal' brain tissue.

(Colvin *et al*., 2008). An extension of DWI is diffusion tensor imaging (DTI) which obtains multidirectional images that can be used to obtain diffusional directionality information quantified as fractional anisotropy and displayed as dominant white fiber tract maps (tractography) ((Waldman *et al*., 2009). DTI was used to differentiate between two rat glioma models, which observed C6 glioma-induced ischemia of tumor-surrounding tissues, compared to the more infiltrative nature of F98 gliomas that penetrated into the corpus callosum (Asanuma *et al*., 2008a, 2008b).

Arterial spin labeling (ASL), a perfusion-weighted MRI method, uses a MR image signal based on the influx of magnetically labeled water into blood, as a means of quantifying absolute levels of cerebral blood flow (CBF) (Waldman *et al*., 2009). Another widely used perfusion method is dynamic susceptibility contrast MRI (DSC-MRI), which can be used to measure relative cerebral blood volume, relative cerebral blood flow (rCBF) and mean transit time from the kinetics resulting from a change in signal intensity following the bolus administration of a gadolinium (Gd)-based contrast agent (Waldman *et al*., 2009). Steady-state susceptibility contrast (SSC) images were used to obtain MRI vessel caliber index (VCI) measurements in a xenograft orthotopic U87 mouse brain tumor model, and were found to correlate closely with intravital optical microscopy (IVM) measurements (Farrar *et al*., 2010). Dynamic contrast-enhanced MRI (DCE-MRI) is commonly used to measure the permeability of the blood-brain-barrier (BBB). The transfer coefficient, K^{trans} is associated with endothelial permeability, vascular surface area and blood flow ((Waldman *et al*., 2009). DCE-MRI revealed a significant change in tumor vessel permeability that was dependent on tumor progression and size in a GL26 orthotopic mouse glioblastoma model (Veeravagu *et al*., 2008). Fig. 5C depicts decreased perfusion values in a C6 glioma, compared to contralateral 'normal' brain tissue, obtained using the ASL method. Perfusion values were found to be increased in the more aggressive RG2 rat glioma compared to C6 (Towner *et al*., 2010a), which is associated with increased vascular proliferation in this model. The increased perfusion in the RG2 model was also correlated with increased capillary vascularity visualized in 3D confocal microscopy fluorescence images, as well as more diffuse and smaller blood vessels observed by MRA, compared to the C6 model (Towner *et al*., 2010a). A study by Valable *et al*. demonstrated that there was a slight reduction in vessel density in the tumor center within RG2 gliomas compared to a more increased reduction in vessel density within C6 gliomas, which was characterized by an increased blood volume fraction, and a

smaller relative increase in vessel size index in the RG2 tumor (Valable *et al*., 2008). The vessel density eventually decreased with increasing tumor cell proliferation (Valable *et al*., 2008). It was thought that early expression of Ang-2, MMP-2 and MMP-9, which has been found in C6 gliomas, could account for the destabilization of vessel walls and a reduction in vessel density during C6 tumor growth (Valable *et al*., 2008).

5.3 Tumor metabolism

Magnetic resonance spectroscopy (MRS) is an MR method that allows regional metabolite levels to be measured in tumors compared to surrounding non-tumor tissue. Important metabolites that can be assessed by ^{1}H-MRS in brain tumors include N-acetyl aspartate (NAA), total creatine (tCr), total choline (tCho), lactate, *myo*-inositol and mobile lipids associated with necrosis. Metabolite levels can be quantified as metabolite ratios or absolute concentrations, or analyzed using pattern recognition (Waldman *et al*., 2009). Figure 6 depicts an example of regional MR spectra obtained in a rat C6 glioma within tumor and contralateral 'normal' brain tissues. Glioma tissue has characteristic increased mobile lipid signals at 1.3 and 0.9 ppm, as well as decreased NAA, tCr and tCho, compared to surrounding 'normal' brain tissue. Metabolites measured by MRS can provide information on brain tissue status, such as (1) NAA being a marker of healthy neuronal integrity, which is compromised within brain tumors, (2) choline-containing compounds being associated with cell membrane turnover, (3) creatine-containing compounds being associated with the cellular energy status, (4) lactate being linked to anaerobic respiration, and (5) mobile lipids resulting from intracellular lipid droplets and necrosis (Waldman *et al*., 2009). Spatially resolved ^{1}H-MRS was used to reveal significantly decreased levels of NAA and tCr and increased lactate (or lipids) in intracerebral rat C6 gliomas, compared to the contralateral hemisphere (Ross *et al*., 1992; Terpstra *et al*., 1996). In F98 rat gliomas there were detected increases in tCho, *myo*-inositol and lipids, as well as the absence of a NAA signal (Gyngell *et al*., 1994).

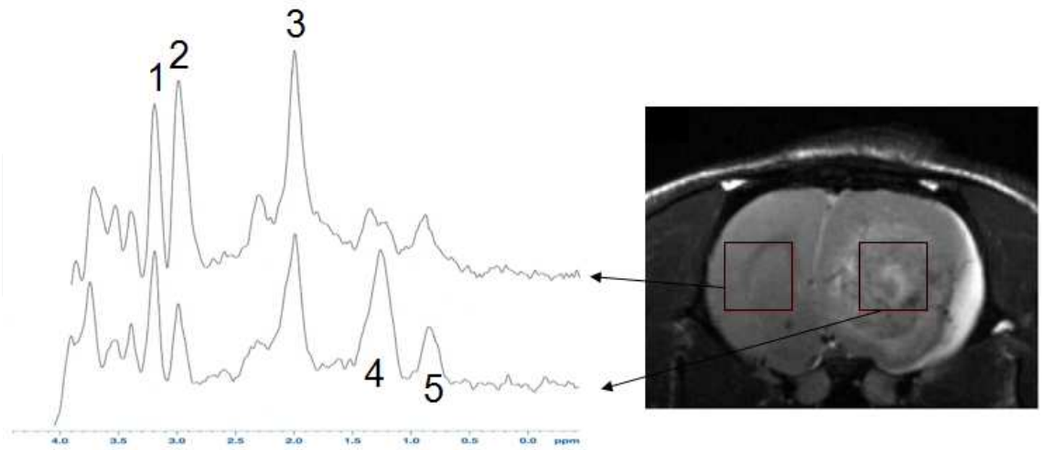

Fig. 6. MR spectroscopy of a rat C6 glioma. Regional (PRESS; point-resolved spectroscopy; 3×3×3 mm^3 or 27 µl volume) was obtained in tumor (right region in T_2-weighted; bottom spectrum) and 'normal' (left region; top spectrum) brain tissues (19 days post-intracerebral implantation of C6 cells). Peak assignments: (1) tCho (total choline), (2) tCr (total creatine), (3) NAA (N-acetyl aspartate), (4) methylene $(-CH_2-)_n$ lipid hydrogens, and (5) methyl $(-CH_3)$ lipid hydrogens.

Other atomic nuclei, other than ^{1}H, have also been used to assess ^{13}C and ^{19}F containing compounds in rodent gliomas. Hyperpolarized ^{13}C MR metabolic imaging was used to follow the metabolism of hyperpolarized [1-(13)C]-pyruvate to lactate in rats with human glioblastoma xenografts (U-251 MG and U-87 MG), indicating higher levels in tumor versus normal brain tissue, and variations between tumor models (Park *et al*., 2010). Rat 9L glioma cells labeled with perfluoro-15-crown-5-ether *ex vivo* and implanted into rat striatum was used to measure intracellular partial pressure of oxygen (pO_2) (oximetry) in tumors (Kadayakkara *et al*., 2010).

5.4 Molecular imaging

The concept used in molecular imaging is to couple a targeting moiety (antibody or peptide targeted to a protein of interest) to a reporter molecule, such as a MRI contrast agent. Two commonly used MRI contrast agents are gadolinium (Gd)-based compounds, or iron oxide-based nanoparticles. The targeted MR probes are often injected via a tail-vein in rats or mice. The expression of cell adhesion molecules, such as integrins, has been found to be up-regulated during tumor growth and angiogenesis, and $\alpha_V\beta_3$ expression which has been correlated with tumor aggressiveness, can be measured by MRI with targeted paramagnetic-labeled cyclic arginine-glycine-aspartic acid (RGD) peptides (Sipkins *et al*., 1998; Waerzeggers *et al*., 2010). Within U87MG xenograft tumors in nude mice, RGD-labeled ultrasmall superparamagnetic iron oxide (USPIO) probes were found to accumulate only within the neovasculature associated with tumors, but not within tumor cells (Kiessling *et al*., 2009). Tumor angiogenesis was also monitored via the expression of CD105 in F98 tumor-bearing rats with the use of Gd-DTPA liposomes targeted to CD105 (CD105-Gd-SLs) and MR imaging (Zhang *et al*., 2009). Combined MRI-coupled fluorescence tomography was used to assess epidermal growth factor receptor (EGFR) status in high- and low-EGFR expression tumor cells injected into nude mice by measuring the levels of a near-infrared fluorophore bound to a EGF ligand (Davis *et al*., 2010).

MR imaging probes have also been developed to monitor *in vivo* levels of other angiogenic proteins known to be over-expressed in malignant brain tumors, such as VEGF-R2 (vascular endothelial growth factor receptor 2) (He *et al*., 2010; Towner *et al*., 2010b); a tumor cell migration/invasion marker, such as c-Met, a tyrosine kinase receptor for the scatter factor (also known as the hepatocyte growth factor) (Towner *et al*., 2008, 2010c); and the inflammatory marker, inducible nitric oxide synthase (iNOS) (Towner *et al*., 2010a). With the use of a Gd-DTPA-albumin-anti-VEGFR2-biotin probe, regional differences in VEGFR2 levels were detected by MRI *in vivo* in a C6 glioma model, and probe-specificity for glioma tissue, particularly in the peri-tumor and peri-necrotic regions, was confirmed by tagging the biotin moiety of the probe in excised tissues with streptavidin-Cy3 (He *et al*., 2010). The control non-specific probe had rat IgG conjugated to the albumin, instead of the VEGFR2 antibody. A similar result was obtained when an aminated dextran-coated iron-oxide nanoparticles conjugated with a VEGFR2 antibody was used in a C6 glioma model, where distribution of the probe was mainly in the peri-tumor and peri-necrotic regions of the tumor (He *et al*., 2010). Confirmation of the presence of the nanoprobes was obtained by using Prussian blue stain for the VEGFR2-targeting iron oxide nanoparticles in excised tumor tissues (He *et al*., 2010).

Both Gd- and iron oxide-based probes were also developed to characterize c-Met levels in C6 gliomas. c-Met is a tumor marker that is over-expressed in many malignant cancers,

indicative of the invasive nature of a tumor. The distribution of c-Met was found to be more widely dispersed, but mainly concentrated in peri-tumor regions (Towner *et al*., 2008, 2010c). Figure 7A depicts the contrast-enhancement in a C6 glioma 3 hours following i.v. administration of a Gd-DTPA-albumin-anti-c-Met-biotin probe, and the corresponding perfusion map showing the increased uptake of the anti-c-Met probe in the peri-tumor regions (Towner *et al*., 2008).

iNOS levels were found to vary in different rat glioma models, as detected with a Gd-DTPA-albumin-anti-iNOS-biotin (anti-iNOS) probe, where percent MRI signal intensity changes were highest in the C6 tumor, compared to the RG2 and ENU-induced tumors (Towner *et al*., 2010a). Dynamic kinetic monitoring of the anti-iNOS probe indicated sustained uptake over 3 hours within tumor tissue regions, and no specific uptake of a control Gd-DTPA-albumin-IgG-biotin contrast agent within tumors (Towner *et al*., 2010a). Fluorescence imaging of the anti-iNOS probe by targeting the biotin moiety with streptavidin-Cy3, verified higher levels of probe uptake in C6 tumors versus RG2 gliomas, despite the increased perfusion and micro-vascularity detected in the RG2 tumors (Towner *et al*., 2010a). Confirmation of the presence of iNOS in glioma cell membrane, but not in normal astrocytes, was obtained by transmission electron microscopy of gold-labeled anti-iNOS antibodies (Towner *et al*., 2010a).

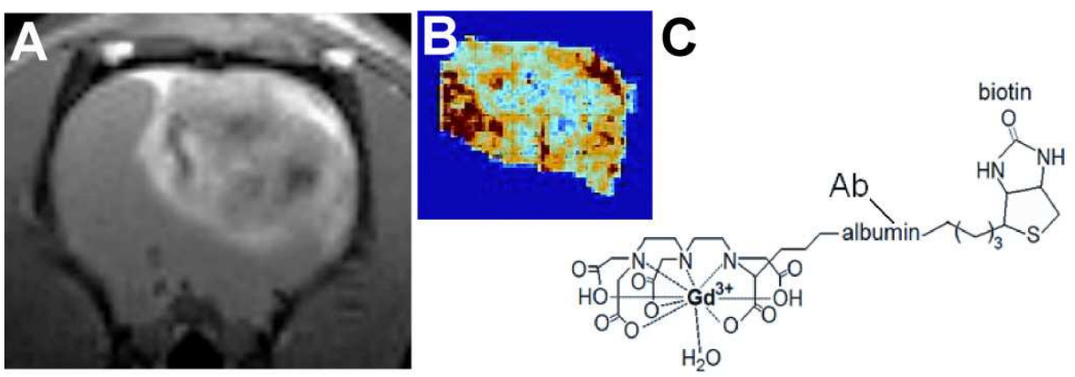

Fig. 7. Molecular MR imaging of c-Met levels in a rat C6 glioma. (A) T_1-weighted MR image 3 hours following i.v. administration of a Gd-DTPA-albumin-anti-c-Met-biotin probe. Note contrast enhancement in peri-tumor regions. (B) Perfusion map depicting distribution of the anti-c-Met probe. (C) Illustration of the Gd-DTPA-albumin-anti-c-Met-biotin probe, with the antibody (Ab) conjugated to albumin.

6. MRI evaluation of therapeutics against gliomas

Clinically, therapeutic response to surgical resection of gliomas, followed by radiation and chemotherapy, can be assessed by dynamic contrast-enhanced morphological MRI, increases in ADC values detected by DWI (Waerzeggers *et al*., 2010), decreases in the fractional tumor volume with a corresponding low relative cerebral blood volume detected by perfusion imaging, and/or reduced choline levels detected by MRS (Waldman *et al*., 2009). DCE-MRI was used to establish reduced Gd enhancement consistent with decreased vascular permeability following i.v. bevacizumab and carboplatin therapy in a human glioma (UW28) nude rat model (Jahnke *et al*., 2009). DCE-MRI using a high molecular weight contrast agent, albumin-Gd-DTPA, showed significantly increased K^{trans} at the rim of

a VEGFR tyrosine kinase inhibitor (Vetanalib, PTK787) (anti-angiogenic) treated U251 gliomas in rats (Ali *et al*., 2010). Low-molecular-weight (Gd-DOTA; gadoterate meglumine) and macromolecular (P846, 3.5 kDa) MR contrast-enhanced imaging was used to assess the therapeutic effect of an anti-angiogenic compound, sorafenic, and microbeam radiation therapy in a 9L gliosarcoma model, finding that anti-angiogenic therapy decreased tumor vessel permeability to the macromolecular contrast agent (Lemasson *et al*., 2010). Dynamic perfusion MRI using iron oxide nanoparticles (ferumoxytol) was used to assess the vascular effects of an anti-angiogenic agent versus corticosteroid (dexamethasone) treatment in a U87MG human glioma model in athymic rats, which found that bevacizumab significantly decreased the tumor blood volume and decreased permeability as determined by an increased time-to-peak enhancement (Varallyay *et al*., 2009).

Morphological MRI, MR angiography and perfusion imaging were used to assess the therapeutic efficacy of nitrone-based compounds as anti-glioma agents in a rat C6 glioma model. It was demonstrated that the nitrone, α-phenyl-*tert*-butyl nitrone (PBN) was able to prevent and/or decrease tumor volumes (by ~60-fold, with significance, $p<0.001$), increase animal survival (>90%), and decrease total tumor blood volumes (by ~20%), in comparison to non-treated rats bearing C6 gliomas (Doblas *et al*., 2008). Another cohort of rats were intracerebrally implanted with C6 glioma cells, monitored for tumor growth, and when tumors reached a volume of ~50 mm^3 (approximately at 15 days post-intracerebral implantation of C6 glioma cells), PBN was administered (drinking water, 0.065% w/v) for a period of 25 days (Doblas *et al*., 2008). In the post-tumor treatment group, PBN was found to increase survival (40% of the treated rats, $p<0.05$), and decrease tumor volumes by ~2-fold, but was found to be non-significant (Doblas *et al*., 2008). Regarding post-tumor treatment, PBN was also found to not significantly affect blood tumor volumes, compared to non-treated rats (Doblas *et al*., 2008). It was concluded from these studies that PBN, when administered prophylactically, may have an effect on angiogenesis (Doblas *et al*., 2008).

Conversely, rats post-tumor treated with a PBN-derivative, OKN-007, were found to have significantly decreased tumor volumes (~3-fold, $p<0.05$), decreased the apparent diffusion coefficients (ADC) (~20%, $p<0.05$), and increased tissue perfusion rates (~60%, $p<0.05$) in tumors, compared to non-treated rats (Garteiser et al., 2010). OKN-007 was administered in the drinking water at 10 mg/kg/day starting when tumors had reached ~50 mm^3 in volume (about day 15 following intracerebral implantation of rat C6 glioma cells), and continued for a total of 10 days (Garteiser *et al*., 2010). One group of rats was euthanized after the 10 day treatment period, and a second group was monitored for an additional 25 days following the treatment period (Garteiser *et al*., 2010). In the cohort of animals that were treated for 10 days and then euthanized, percent survival was 100% ($p<0.0001$), whereas for the rats that were monitored for an additional 25 days the percent survival was greater than 80% ($p<0.001$) (Garteiser *et al*., 2010). Morphological MRI was used to calculate tumor volumes; diffusion-weighted imaging (DWI) was used to measure ADC, which assesses changes in water diffusion due to tissue structural alterations; and perfusion-weighted MRI (pMRI) was used to characterize tissue perfusion rates, which can provide information on alterations in the vascular capillary bed. Currently, the known pharmacological effects of the nitrones are primarily anti-inflammatory in nature. The parent nitrone compound, PBN, is known to inhibit (1) cyclooxygenase-2 (COX-2), (2) inducible nitric oxide synthase (iNOS), and (3) nuclear factor kappaB (NF-κB) (Floyd *et al*., 2008).

ADC values have been found to increase particularly in the early phase of anticancer therapies (Waerzeggers *et al*., 2010). Increases in ADC were found to be a time and dose sensitive marker of tumor (mouse xenografts) response to radiation therapy (Larocque *et al*., 2009). Contrast-enhanced MRI and DWI were used to characterize the vascular and cellular responses of GL261 and U87 gliomas to the tumor-vascular disrupting agent (VDA) 5,6-dimethylxanthenone-4-acetic acid (DMXAA), which indicated significantly increased ADC values and the accumulation of contrast agent in treated tumors (Seshadri and Ciesielski, 2009). ADC and 3D T_2*-weighted MRI measurements were used to validate ZD6474 (tyrosine kinase receptor inhibitor) inhibition on tumor growth and angiogenesis in EGFRvIII-expressing GBM8 gliomas (Yiin *et al*., 2010).

In a gene therapy-induced apoptosis (ganciclovir-treated herpes simplex thymidine kinase (HSV-tk) gene-transfected BT4C gliomas) study, combined DWI and ^{1}H-MRS assessment was used to find interconnecting trends following therapeutic response in water diffusion and water-referenced concentrations of mobile lipids (Liimatainen *et al*., 2009). It is thought that apoptosis leads to an increase in ^{1}H-MRS detectable mobile cholesterol compounds and unsaturated lipids resulting from the gene therapy-induced apoptosis (Hakumäki et al., 1999; Liimatainen *et al*., 2006, 2009). Amide proton transfer (APT) MRI was recently used to differentiate between different glioma models (SF188/V$^+$ glioma and 9L gliosarcoma) and radiation-induced necrosis, where viable glioma tissue was hyperintense and radiation necrosis was hypointense to isointense (Zhou *et al*., 2011).

Iron oxide-based nanoparticles have recently been used as cell tracking agents, or non-targeted or targeted drug delivery. Magnetically-labeled cytotoxic T-cells were used as cellular probes and tracked by T_2- and T_2*-weighted MRI to differentiate glioma tissue from focal radiation necrosis in U-251 glioma-bearing rodents (Arbab *et al*., 2010). Focused ultrasound, which was used to permeabilize the blood-brain barrier and increase passive diffusion, was found to increase the delivery of drug (1,3-bis(2-chloroethyl)-1-nitrosourea and iron oxide nanoparticles that can be monitored with MRI, in a rat C6 glioma model (Chen *et al*., 2010). EGFRvIII antibody-conjugated iron oxide nanoparticles were used for convection-enhanced delivery and targeted therapy in glioblastoma mouse xenografts (U87DeltaEGFRvIII), and assessed by T_2-weighted MRI (Hadjipanayis *et al*., 2010).

7. Conclusions

There are several orthotopic rodent glioma models that have been used for several decades, and more recent transgenic, orthotopic xenograft neurosphere- or PDGFB-expressing virus-induced models that better reflect the genetic and stem-cell involvement in glia tumorigenesis. It is important that appropriate glioma models are used that best represent our current knowledge of malignant glioblastomas in humans. Ideally the more recent models should be used if possible, however if an orthotopic syngeneic model is required, then the rat F98 or RG2, and mouse GL26(1) models seem to have some characteristics that resemble aspects of human glioblastomas, such as vascular proliferation, and aggressive and infiltrative tumor growth. The human U87 MG glioma cell xenograft model in athymic rodents also has beneficial characteristics resembling some aspects of human GBM. Choosing an appropriate model is particularly important when evaluating new anti-glioma therapies, as these models need to consider recurrent gliomas, possibly derived from cancer stem cells, which are radiation- and chemotherapy-resistant, and currently reflect the poor prognosis of high-grade gliomas in humans.

The evaluation of critical changes during tumorigenesis, as well as monitoring therapeutic responses, requires the use of appropriate imaging technologies. The focus of this review has been on the use of MR imaging and spectroscopy methodologies in pre-clinical rodent models for gliomas, many of which translate to clinical applications. DCE-MRI and ASL perfusion imaging, and MRA, can provide valuable information regarding morphological and dynamic alterations associated with tumor vasculature or angiogenesis. The ADC, as measured by DWI, and DTI, can assess tissue structural and organizational changes that occur during tumor formation. MR spectroscopy provides metabolic markers, such as NAA, tCr, tCho, lactate, and mobile lipids that undergo significant changes in concentrations during glial tumorigenesis, as a result of neuronal degradation (NAA), cell proliferation (tCho), anaerobic respiration (lactate), and necrosis (mobile lipids). These MRI-observable changes, such as tumor ADC, rCBF, K^{trans}, cerebral blood volume, and ^{1}H-MRS detectable metabolites, can all be important criteria to assess therapeutic efficacy. Molecular MRI (mMRI) is a targeted approach that can be used to assess specific tumor molecular markers associated with angiogenesis, apoptosis, cell migration/invasion, metastasis, proliferation, or inflammation. Targeted probes can also be used to deliver therapeutic compounds to tumors that express high levels of a specific molecular marker, and if these probes have a Gd-, manganese (Mn)- or iron oxide-based construct, then they can be monitored by MRI.

8. References

Alexiou, G.A. & Voulgaris S. (2010) The role of the PTEN gene in malignant gliomas. *Neurol. Neurochir. Pol.*, 44(1): 80-6. ISSN:0028-3843

Ali, M.M., Janic, B., Babajani-Feremi, A., Varma, N.R., Iskander, A.S., Anagli, J. & Arbab, A.S. (2010) Changes in vascular permeability and expression of different angiogenic factors following anti-angiogenic treatment in rat glioma. *PLoS One*, 15;5(1):e8727. ISSN:1932-6203

Arbab, A.S., Janic, B., Jafari-Khouzani, K., Iskander, A.S., Kumar, S., Varma, N.R., Knight, R.A., Soltanian-Zadeh, H., Brown, S.L. & Frank, J.A. (2010) Differentiation of glioma and radiation injury in rats using *in vitro* produce magnetically labeled cytotoxic T-cells and MRI. *PLoS One*, 26;5(2):e9365. ISSN:1932-6203

Asanuma, T., Doblas, S., Tesiram, Y.A., Saunders, D., Cranford, R., Pearson, J., Abbott, A., Smith, N. & Towner, R.A. (2008a) Diffusion tensor imaging and fiber tractography of C6 rat glioma. *J. Magn. Reson. Imaging*, 28(3): 566-573. ISSN:1053-1807

Asanuma, T., Doblas, S., Tesiram, Y.A., Saunders, D., Cranford, R., Yasui, H., Inanami, O., Smith, N., Floyd, R.A., Kotake, Y. & Towner, R.A. (2008b) Visualization of the protective ability of a free radical trapping compound against rat C6 and F98 gliomas with diffusion tensor fiber tractography. *J. Magn. Reson. Imaging*, 28(3): 574-587. ISSN:1053-1807

Assanah, M., Lochhead, R., Ogden, A., Bruce, J., Goldman, J. & Canoll, P. (2006) Glial progenitors in adult white matter are driven to form malignant gliomas by platelet-deived growth factor-expressing retroviruses. *J. Neurosci.*, 26(25): 6781-6790. ISSN:0270-6474

Assanah, M.C., Bruce, J.N., Suzuki, S.O., Chen, A., Goldman, J.E. & Canoll, P. (2009) PDGF stimulates the massive expansion of glial progenitors in the neonatal forebrain. *Glia*, 57(16): 1835-1847. ISSN:0894-1491

Barth, R.F. (1998) Rat brain tumor models in experimental neuro-oncology: the 9L, C6, T9, F98, RG2 (D74), RT-2 and CNS-1 gliomas. *J Neurooncol.,* 36(1): 91-102. ISSN:0167-594X

Barth, R.F. & Kaur, B. (2009) Rat brain tumor models in experimental neuro-oncology: the C6, 9L, T9, RG2, F98, BT4C, RT-2 and CNS-1 gliomas. *J. Neurooncol.,* 94(3): 299-312. ISSN:0167-594X

Calzolari, F. & Malatesta, P. (2010) Recent insights into PDGF-induced gliomagenesis. *Brain Pathol.,* 20(3): 527-38. ISSN:1015-6305

Central Brain Tumor Registry of the United States (CBTRUS). 2011 CBTRUS Statistical Report: Primary Brain and Central Nervous System Tumors Diagnosed in the United States in 2004-2007. http://www.cbtrus.org/2011-NPCR-SEER/WEB-0407-Report-3-3-2011.pdf. pp. 54-57.

Chen, P.Y., Liu, H.L., Hua, M.Y., Yang, H.W., Huang, C.Y., Chu, P.C., Lyu, L.A., Tseng, I.C., Feng, L.Y., Tsai, H.C., Chen, S.M., Lu, Y.J., Wang, J.J., Yen, T.C., Ma, Y.H., Wu, T., Chen, J.P., Chuang, J.I., Shin, J.W., Hsueh, C. & Wei, K.C. (2010) Novel magnetic/ultrasound focusing system enhances nanoparticles drug delivery for glioma treatment. *Neuro. Oncol*., 12(10): 1050-60. ISSN:1522-8517

Cheng, S.Y., Huang, H.J., Nagane, M., Ji, X.D., Wang, D., Shih, C.C., Arap, W., Huang, C.M. & Cavenee, W.K. (1996) Suppression of Glioblastoma Angiogenicity and Tumorigenicity by Inhibition of Endogenous Expression of Vascular Endothelial Growth Factor. *Proc. Natl. Acad. Sci. U. S. A.*, 93(16): 8502-8507. ISSN:0027-8424

Chinnam, M. & Goodrich, D.W. (2011) RB1, development, and cancer. *Curr. Top. Dev. Biol.*, 94: 129-69. ISSN:0070-2153

Colvin, D.C., Yankeelov, T.E., Does, M.D., Yue, Z., Quarles, C. & Gore, J.C. (2008) New insights into tumor microstructure using temporal diffusion spectroscopy. *Cancer Res*., 68 (14): 5941-7. ISSN:0008-5472

Davaki, P. & Lantos, P.L. (1980) Morphological analysis of malignancy: a comparative study of transplanted brain tumors. *Br. J. Exp. Pathol.,* 61(6): 655-60. ISSN:0007-1021

Davis, S.C., Samkoe, K.S., O'Hara, J.A., Gibbs-Strauss, S.L., Payne, H.L., Hoopes, P.J., Paulsen, K.D. & Pogue, B.W. (2010) MRI-coupled fluorescence tomography quantifies EGFR activity in brain tumors. *Acad. Radiol*. 17 (3): 271-6. ISSN:1076-6332

De Vries, N.A., Bruggeman, S.W., Hulsman, D., de Vries, H.I., Zevenhoven, J., Buckle, T., Hamans, B.C., Leenders, W.P., Beijnen, J.H., van Lohuizen, M., Berns, A.J.M. & van Tellingen, O. (2010) Rapid and robust transgenic high-grade glioma mouse models for therapy intervention studies. *Clin. Cancer Res.*, 16(13): 3431-3441. ISSN:1078-0432

Doblas, S., Saunders, D., Kshirsagar, P., Pye, Q., Oblander, J., Gordon, B., Kosanke, S., Floyd, R.A. & Towner, R.A. (2008) Phentyl-tert-butyl nitrone induces tumor regression and decreases angiogenesis in a C6 rat glioma model. *Free Radical Biology & Medicine*, 44(1): 63-72. ISSN:0891-5849

Doblas, S., He, T., Saunders, D., Pearson, J., Hoyle, J., Smith, N., Lerner, M. & Towner, R.A. (2010) Glioma morphology and tumor-induced vascular alterations revealed in seven glioma models by in vivo magnetic resonance imaging and angiography. *J. Magn. Reson. Imaging,* 32(2): 267-275. ISSN:1053-1807

Drogat, B., Auguste, P., Nguyen, D.T., Bouchecareilh, M., Pineau, R., Nalbantoglu, J., Kaufman, R.J., Chevert, E., Bikfalvi, A. & Moenner, M. (2007) IRE1 signaling is essential for ischemia-induced vascular endothelial growth factor-A expression and

contributes to angiogenesis and tumor growth *in vivo*. *Cancer Res.,* 67(14): 6700-07. ISSN:0008-5472

Farrar, C.T., Kamoun, W.S., Ley, C.D., Kim, Y.R., Kwon, S.J., Dai, G., Rosen, B.R., di Tomaso, E., Jain, R.K. & Sorensen, A.G. (2010) In vivo validation of MRI vessel caliber index measurement methods with intravital optical microscopy in a U87 mouse brain tumor model. *Neuro. Oncol.*, 12 (4): 341-50. ISSN:1522-8517

Fei, X.F., Zhang, Q.B., Dong, J., Diao, Y., Wang, Z.M., Li, R.J., Wu, Z.C., Wang, A.D., Lan, Q., Zhang, S.M. & Huang, Q. (2010) Development of clinically relevant orthotopic xenograft mouse model of metastatic lung cancer and glioblastoma through surgical tumor tissues injection with trocar. *J. Exp. Clin. Cancer Res.*, 29: 84. ISSN:0392-9078

Floyd, R.A., Kopke, R.D., Choi, C.-H., Foster, S.B., Doblas, S. & Towner, R.A. (2008) Nitrones as therapeutics. *Free Radical Biology & Medicine*, 45(10): 1361-1374. ISSN:0891-5849

Garteiser, P., Doblas, S., Watanabe, Y., Saunders, D., Hoyle, J., Lerner, M., He, T., Floyd, R.A. & Towner, R.A. (2010) Multiparametric assessment of the anti-glioma properties of OKN007 by magnetic resonance imaging. *J. Magnetic Resonance Imaging*, 31(4): 796-806. ISSN:1053-1807

Grobben, B., De Deyn, P.P. & Slegers, H. (2002) Rat C6 glioma as experimental model system for the study of glioblastoma growth and invasion. *Cell Tissue Res.,* 310(3): 257-270. ISSN:0302-766X

Groothuis, D.R., Fischer, J.M., Pasternak, J.F., Blasberg, R.G., Vick, N.A. & Bigner, D.D. (1983) Regional measurements of blood-to-tissue transport in experimental RG-2 rat gliomas. *Cancer Res.,* 43(7): 3368-3373. ISSN:0008-5472

Gudinaviciene, I., Pranys, D. & Juozaityte, E. (2004) Impact of morphology and biology on the prognosis of patients with gliomas. *Medicina (Kaunas),* 40(2): 112-120. ISSN:1010-660X

Gyngell, M.L., Hoehn-Berlage, M. & Hossmann, K.A. (1994) Proton MR spectroscopy of experimental brain tumors *in vivo*. *Acta Neurochir. Suppl. (Wien)*, 60: 350-2. ISSN:0065-1419

Hadjipanayis, C.G., Machaidze, R., Kaluzova, M., Wang, L., Schuette, A.J., Chen, H., Wu, X. & Mao, H. (2010) EGFRvIII antibody-conjugated iron oxide nanoparticles for magnetic resonance imaging-guided convection-enhanced delivery and targeted therapy of glioblastoma. *Cancer Res.*, 70(15):6303-12. ISSN:0008-5472

Hakumäki, J., Poptani, H., Sandmair, A.-M., Ylä-Herttuala, S. & Kauppinen, R.A. (1999) 1H MRS detects polyunsaturated fatty acid accumulation during gene therapy of glioma: implications for the in vivo detection of apoptosis. *Nature Medicine*, 5 (11) 1323-1327. ISSN:1078-8956

He, T., Smith, N., Saunders, D., Doblas, S., Watanabe, Y., Hoyle, J., Silasi-Mansat, R., Lupu, F., Lerner, M., Brackett, D.J. & Towner, R.A. (2010) Molecular MRI assessment of vascular endothelial growth factor receptor-2 in rat C6 gliomas. *J. Cell. Mol. Med.* In press. 1582-4934

Hede, S.-M., Hansson, I., Afink, G.B., Eriksson, A., Nazarenko, I., Andrae, J., Genove, G., Westermark, B. & Nister, M. (2009) GFAP promoter driven transgenic expression of PDGFB in the mouse brain leads to glioblastoma in a Trp53 null background. *Glia,* 57(11): 1143-1153. ISSN:0894-1491

Jacques, T.S., Swales, A., Brzozowski, M.J., Henriquez, N.V., Linehan, J.M., Mirzadeh, Z., O'Malley, C., Naumann, H., Alvarez-Buylla, A. & Brandner, S. (2010) Combinations of genetic mutations in the adult neural stem cell compartment determine brain tumor phenotypes. *The EMBO Journal,* 29(1): 222-235. ISSN:0261-4189

Jahnke, K., Muldoon, L.L., Varallyay, C.G., Lewin, S.J., Kraemer, D.F. & Neuwelt, E.A. (2009) Bevacizumab and carboplatin increase survival and asymptomatic tumor volume in a glioma model. *Neuro. Oncol*., 11 (2): 142-50. ISSN:1522-8517

Kadayakkara, D.K., Janjic, J.M., Pusateri, L.K., Young, W.B. & Ahrens, E.T. (2010) In vivo observation of intracellular oximetry in perfluorocarbon-labeled glioma cells and chemotherapeutic response in the CNS using fluorine-19 MRI. *Magn. Reson. Med*., 64 (5): 1252-9. ISSN:0740-3194

Kauppinen, R.A. (2002) Monitoring cytotoxic tumor treatment response by diffusion magnetic resonance imaging and proton spectroscopy. *NMR Biomed*., 15 (1): 6-17. ISSN:0952-3480

Kiessling, F., Huppert, J., Zhang, C., Jayapaul, J., Zwick, S., Woenne, E.C., Mueller, M.M., Zentgraf, H., Eisenhut, M., Addadi, Y., Neeman, M. & Semmler, W. (2009) RGD-labeled USPIO inhibits adhesion and endocytototic activity of alpha v beta3-integrin-expressing glioma cells and only accumulates in the vascular tumor compartment. *Radiology*, 253 (2): 462-9. ISSN:0033-8419

Kim, D.H., Kundu, J.K. & Surh, Y.J .(2011) Redox modulation of p53: Mechanisms and functional significance. *Mol. Carcinog.,* 50(4): 222-34. ISSN:0899-1987

Kish, P.E., Blaivas, M., Strawderman, M., Muraszko, K.M., Ross, D.A., Ross, B.D. & McMahon, G. (2001) Magnetic resonance imaging of ethyl-nitrosourea-induced rat gliomas: a model for experimental therapeutics of low-grade gliomas. *J. Neurooncol*., 53(3): 243-257. ISSN:0167-594X

Koestner, A., Swenberg, J.A. & Wechsler, W. (1971) Transplacental production with ethylnitrosourea of neoplasms of the nervous system in Sprague-Dawley rats. *Am. J. Pathol*., 63(1):37-56. ISSN:0002-9440

Koestner, A. (1990) Characterization of N-nitrosourea-induced tumors of the nervous system; their prospective value for studies of neurocarcinogenesis and brain tumor therapy. *Toxicologic pathology,* 18(1 Pt 2): 186-192. ISSN:0192-6233

Larocque, M.P., Syme, A., Yahya, A., Wachowicz, K., Allaunis-Turner, J. & Fallone, B.G. (2009) Temporal and dose dependence of T2 and ADC at 9.4 T in a mouse model following single fraction radiation therapy. *Med. Phys*., 36 (7): 2948-54.
ISSN:0094-2405

Lemasson, B., Serduc, R., Maisin, C., Bouchet, A., Coquery, N., Robert, P., Le Duc, G., Troprès, I., Rémy, C. & Barbier, E.L. (2010) Monitoring blood-brain barrier status in a rat model of glioma receiving therapy: dual injection of low-molecular-weight and macromolecular MR contrast media. *Radiology*, 257 (2): 342-52. ISSN: 0033-8419

Liimatainen, T., Lehtimäki, K., Ala-Korpela, M. & Hakumäki, J. (2006) Identification of mobile cholesterol compounds in experimental gliomas by 1H MRS in vivo: effects of ganciclovir-induced apoptosis on lipids. *FEBS Letters*, 580(19): 4746-50. ISSN:0014-5793

Liimatainen, T., Hakumäki, J.M., Kauppinen, R.A. & Ala-Korpela, M. (2009) Monitoring of gliomas in vivo by diffusion MRI and (1)H MRS during gene therapy-induced

apoptosis: interrelationships between water diffusion and mobile lipids. *NMR Biomed.*, 22 (3): 272-9. ISSN:0952-3480

Lohmann ,D. (2010) Retinoblastoma. *Adv. Exp. Med. Biol.* 685: 220-7. ISSN:0065-2598

Maclaine, N.J. & Hupp, T.R. (2011) How phosphorylation controls p53. *Cell Cycle*, Mar 15; 10(6). ISSN:1538-4101

Martens, T., Schmidt, N.O., Eckerich, C., Fillbrandt, R., Merchant, M., Schwall, R., Westphal, M. & Lamszus, K. (2006) A novel one-armed anti-c-Met antibody inhibits glioblastoma growth in vivo. *Clin. Cancer Res.,*12(20 Pt 1): 6144-6152.ISSN:1078-0432

Masui, K., Suzuki, S.O., Torisu, R., Goldman, J.E., Canoll, P. & Iwaki, T. (2010) Glial progenitors in the brainstem give rise to malignant gliomas by platelet-derived growth factor stimulation. *Glia*, 58(9): 1050-1065. ISSN:0894-1491

Muller, P.A., Vousden, K.H. & Norman, J.C. (2011) p53 and its mutants in tumor cell migration and invasion. *J. Cell Biol.* 192(2): 209-18. ISSN:0021-9525

Natsume, A., Kinjo, S., Yuki, K., Kato, T., Ohno, M., Motomura, K., Iwami, K. & Wakabayashi, T. (2011) Glioma-initiating cells and molecular pathology: implications for therapy. *Brain Tumor Pathol.* 28(1): 1-12. ISSN:1433-7398

Niclou, S.P., Fack, F. & Rajcevic, U. (2010) Glioma proteomics: status and perspectives. *J. Proteomics* 73(10): 1823-1838. ISSN:1874-3919

Park, I., Larson, P.E., Zierhut, M.L., Hu, S., Bok, R., Ozawa, T., Kurhanewicz, J., Vigneron, D.B., Vandenberg, S.R., James, C.D. & Nelson, S.J. (2010) Hyperpolarized 13C magnetic resonance metabolic imaging: application to brain tumors. *Neuro. Oncol.*, 12 (2): 133-44. ISSN:1522-8517

Plate, K.H., Breier, G., Millauer, B., Ullrich, A. & Risau, W. (1993) Up-Regulation of Vascular Endothelial Growth Factor and its Cognate Receptors in a Rat Glioma Model of Tumor Angiogenesis. *Cancer Res.,* 53(23): 5822-5827. ISSN:0008-5472

Ross, B.D., Merkle, H., Hendrich, K., Staewen, R.S. & Garwood, M. (1992) Spatially localized *in vivo* ^{1}H magnetic resonance spectroscopy of an intracerebral rat glioma. *Magn. Reson. Med.*, 23 (1): 96-108. ISSN:0740-3194

Sadeghi, N., Camby, I., Goldman, S., Gabius, H.J., Baleriaux, D., Salmon, I., Decaesteckere, C., Kiss, R. & Metens, T. (2003) Effect of hydrophilic components of the extracellular matrix on quantifiable diffusion-weighted imaging of human gliomas: preliminary results of correlating apparent diffusion coefficient values and hyaluronan expression level. *Am. J. Roentgenol.*, 181 (1): 235-41. ISSN:0361-803X

Seshadri, M. & Ciesielski, M.J. (2009) MRI-based characterization of vascular disruption by 5,6-dimethylxanthenone-acetic acid in gliomas. *J. Cereb. Blood Flow Metab.*, 29 (8): 1373-82. ISSN:0271-678X

Shih, A.H., Dai, C., Hu, X., Rosenblum, M.K., Koutcher, J.A. & Holland, E.C. (2004) Dose-dependent effects of platelet-derived growth factor-B on glial tumorigenesis. *Cancer Res.*, 64(14): 4783-4789. ISSN:0008-5472

Shih, A.H. & Holland, E.C. (2006) Platelet-derived growth factor (PDGF) and glial tumorigenesis. *Cancer Lett.,* 232(2): 139-47. ISSN:0304-3835

Sibenaller, Z.A., Etame, A.B., Ali, M.M., Barua, M., Braun, T.A., Casavant, T.L. & Ryken, T.C. (2005) Genetic characterization of commonly used glioma cell lines in the rat animal model system. *Neurosurg. Focus,* 19(4): E1-E9. ISSN:1092-0684 (Electronic)

Sipkins, D.A., Cheresh, D.A., Kazemi, M.R., Nevin, L/M., Bednarski, M.D. & Li, K.C. (1998) Detection of tumor angiogenesis *in vivo* by alphaVnbeta3-targeted magnetic resonance imaging. *Nat. Med*., 4 (5): 623-626. ISSN:1078-8956

Szatmari, T., Lumniczky, K., Desaknai, S., Trajcevski, S., Hidvegi, E.J., Hamada, H. & Safrany, G. (2006) Detailed characterization of the mouse glioma 261 tumor model for experimental glioblastoma therapy. *Cancer Science,* 97(6): 546-553. ISSN:1347-9032

Terpstra, M., High, W.B., Luo, Y., de Graaf, R.A., Merkle, H. & Garwood, M. (1996) Relationship among lactate concentration, blood flow and histopathologic profiles in rat C6 glioma. *NMR Biomed*., 9 (5): 185-94. ISSN:0952-3480

Towner, R.A., Smith, N., Doblas, S., Tesiram, Y., Garteiser, P., Saunders, D., Cranford, R., Silasi-Mansat, R., Herlea, O., Ivanciu, L., Wu, D. & Lupu, F. (2008) *In vivo* detection of c-Met expression in a rat C6 glioma model. *J. Cell. Mol. Med.* 12(1): 174-186. ISSN:1582-1838

Towner, R.A., Smith, N., Doblas, S., Garteiser, P., Watanabe, Y., He, T., Saunders, D., Herlea, O., Silasi-Mansat, R. & Lupu, F. (2010a) In vivo detection of inducible nitric oxide synthase in rodent gliomas. *Free Radic. Biol. Med*., 48(5): 691-703. ISSN:0891-5849

Towner, R.A., Smith, N., Asanao, Y., He, T., Doblas, S., Saunders, D., Silasi-Mansat, R., Lupu, F. & Seeney, C.E. (2010b) Molecular magnetic resonance imaging approaches used to aid in the understanding of angiogenesis *in vivo*: implications for tissue engineering. *Tissue Engineering Part A*, 16 (2) : 357-364). ISSN:1937-3341

Towner, R.A., Smith, N., Asano, Y., Doblas, S., Saunders, D., Silasi-Mansat, R., & Lupu, F. (2010c) Molecular magnetic resonance imaging approaches used to aid in the understanding of the tissue regeneration marker Met *in vivo*: implications for tissue engineering. *Tissue Engineering Part A*, 16 (2) 365-371. ISSN:1937-3341

Valable, S., Lemasson, B., Farion, R, Beaumont, M., Segebarth, C., Remy, C. & Barbier, E.L. (2008) Assessment of blood volume, vessel size, and the expression of angiogenic factors in two rat glioma models : a longitudinal in vivo and ex vivo study. *NMR Biomed*., 21(10): 1043-56. ISSN:0952-3480

Vaquero, J., Coca, S., Zurita, M. , Oya, S., Arias, A., Moreno, M. & Morales, C. (1992) Synaptophysin expression in "ependymal tumors" induced by ethyl-nitrosourea in rats. *Am. J. Pathol*., 141(5):1037-1041. ISSN:0002-9440

Varallyay, C.G., Muldoon, L.L., Gahramanov, S., Wu, Y.J., Goodman, J.A., Li, X., Pike, M.M. & Neuwelt, E.A. (2009) Dynamic MRI using iron oxide nanoparticles to assess early vascular effects of antiangiogenic versus corticosteroid treatment in a glioma model. *J. Cereb. Blood Flow Metab*., 29 (4): 853-60. ISSN:0271-678X

Veeravagu, A., Hou, L.C., Hsu, A.R., Cai, W., Greve, J.M., Chen, X. & Tse, V. (2008) The temporal correlation of dynamic contrast-enhanced magnetic resonance imaging with tumor angiogenesis in a murine glioblastoma model. *Neurol. Res*., 30 (9): 952-9. ISSN:0161-6412

Waerzeggers, Y., Monfared, P., Viel, T., Winkeler, A. & Jacobs, A.H. (2010) Mouse models in neurological disorders: Applications of non-invasive imaging. *Biochimica et Biophysica Acta*, 1802(10): 819-839. ISSN:0006-3002

Waldman, A.D., Jackson, A., Price, S.J., Clark, C.A., Booth, T.C., Auer, D.P., Tofts, P.S., Collins, D.J., Leach, M.O. & Rees, J.H. (2009) Quantitative imaging biomarkers in neuro-oncology. *Nature Reviews Clin. Oncol.*, 6(8): 445-454. ISSN:1759-4774

Wehbe, K., Pineau, R., Eimer, S., Vital, A., Loiseau, H. & Deleris, G. (2010) Differentiation between normal and tumor vasculature of animal and human glioma by FTIR imaging. *Analyst,* 135(12): 3052-9. ISSN:0003-2654

Wei, J., Barr, J., Kong, L.-Y., Wang, Y., Wu, A., Sharma, A.K., Gumin, J., Henry, V., Colman, H., Sawaya, R., Lang, F.F. & Heimberger, A.B. (2010) Glioma-associated cancer-initiating cells induce immunosuppression. *Clin. Cancer Res.*, 16(2): 461-473. ISSN:1078-0432

Weizsaecker, M., Deen, D.F., Rosenblum, M.L., Hoshino, T., Gutin, P.H. & Barker, M. (1981) The 9L Rat Brain Tumor: Description and Application of an Animal Model. *J. Neurol.,* 224(3): 183-192. ISSN:0340-5354

Yiin, J.J., Schornack, P.A., Sengar, R.S., Liu, K.W., Feng, H., Lieberman, F.S., Chiou, S.H., Sarkaria, J.N., Wiener, E.C., Ma, H.I. & Cheng, S.Y. (2010) ZD6474, a multitargeted inhibitor for receptor tyrosine kinases, suppresses growth of gliomas expressing an epidermal growth factor receptor mutant, EGFRvIII, in the brain. *Mol. Cancer Ther.*, 9 (4): 929-41. ISSN:1535-7163

Zhang, D., Feng, X.Y., Henning, T.D., Wen, L., Lu, W.Y., Pan, H., Wu, X. & Zou, L.G. (2009) MR imaging of tumor angiogenesis using sterically stabilized Gd-DTPA liposomes targeted to CD105. *Eur. J. Radiol*., 70 (1): 180-9. ISSN:0720-048X

Zhou, J., Tryggestad, E., Wen, Z., Lai, B., Zhou, T., Grossman, R., Wang, S., Yan, K., Fu, D.X., Ford, E., Tyler, B., Blakeley, J., Laterra, J. & van Zijl, P.C. (2011) Differentiation between glioma and radiation necrosis using molecular magnetic resonance imaging of endogeneous proteins and peptides. *Nature Medicine*, 17(1): 130-4. ISSN:1078-8956

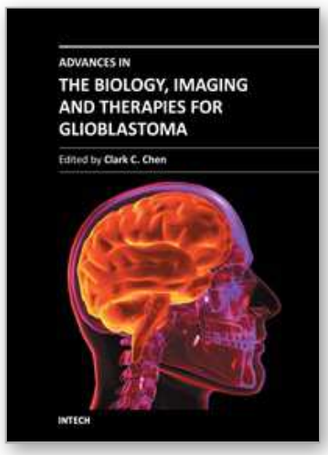

Advances in the Biology, Imaging and Therapies for Glioblastoma
Edited by Prof. Clark Chen

ISBN 978-953-307-284-5
Hard cover, 424 pages
Publisher InTech
Published online 09, November, 2011
Published in print edition November, 2011

This book is intended for physicians and scientists with interest in glioblastoma biology, imaging and therapy. Select topics in DNA repair are presented here to demonstrate novel paradigms as they relate to therapeutic strategies. The book should serve as a supplementary text in courses and seminars as well as a general reference.

How to reference
In order to correctly reference this scholarly work, feel free to copy and paste the following:

Rheal A. Towner, Ting He, Sabrina Doblas and Nataliya Smith (2011). Assessment of Rodent Glioma Models Using Magnetic Resonance Imaging Techniques, Advances in the Biology, Imaging and Therapies for Glioblastoma, Prof. Clark Chen (Ed.), ISBN: 978-953-307-284-5, InTech, Available from: http://www.intechopen.com/books/advances-in-the-biology-imaging-and-therapies-for-glioblastoma/assessment-of-rodent-glioma-models-using-magnetic-resonance-imaging-techniques

INTECH
open science | open minds

InTech Europe
University Campus STeP Ri
Slavka Krautzeka 83/A
51000 Rijeka, Croatia
Phone: +385 (51) 770 447
Fax: +385 (51) 686 166
www.intechopen.com

InTech China
Unit 405, Office Block, Hotel Equatorial Shanghai
No.65, Yan An Road (West), Shanghai, 200040, China
中国上海市延安西路65号上海国际贵都大饭店办公楼405单元
Phone: +86-21-62489820
Fax: +86-21-62489821

IntechOpen